The Efficacy of Taylor's Hypothesis in Aeroacoustic Noise Predictions for Bodies of Revolution

Jarrod T. Banks *, William J. Devenport †
Virginia Tech, Blacksburg, VA, 24060

In turbulence ingestion noise the two point velocity correlation function is a primary input to many analytical acoustic prediction models. As such, methods to determine the form of the two point correlation function in various flow configurations are of vital importance to noise predictions. Often Taylor's hypothesis is assumed in order to relate velocity single point statistics (autocorrelations) to two point correlations (cross-correlations). The applicability of Taylor's frozen flow theorem is examined over the extent of a boundary layer flow generated by an axisymmetric body of revolution inclined at an angle of attack. The decay of the usability of Taylor's frozen flow closer to the wall is examined and the evolution of the two-point correlation structure is shown and compared to existing measurements of an axisymmetric flow. Taylor's frozen flow was found to consistently underpredict the integral length scales by about 10% and its efficacy decay closer to the wall. The correlation structure was found to stretch in the streamwise direction and rotate anti-clockwise as the anchor point was moved towards the wall.

Nomenclature

b	=	blade span
c	=	blade chordlength
c_∞	=	sound speed
D	=	body of revolution diameter (mm)
L_{st}	=	Taylor Integral Lengthscale (mm)
L_s	=	Integral Lengthscale (mm)
r_e	=	distance to observer (m)
S_{pp}	=	sound spectrum (dB/Hz)
$\overline{U}$	=	mean velocity (m/s)
u	=	fluctuating velocity (m/s)
δ	=	boundary layer thickness (mm)

*Graduate Researcher, Department of Aerospace and Ocean Engineering and AIAA Student
†Crofton Professor of Engineering, Center for Research in Experimental Aero/Hydrodynamic Technology, Fellow AIAA

Γ	=	timescales (s)
τ	=	time delay (s)
ρ	=	correlation function
ϕ_{pp}	=	wavenumber spectrum
ω	=	angular frequency (rad/s)

Subscripts

c	=	convection
s	=	streamwise
x,y,z	=	body defined coordinate system

I. Introduction

Turbulent boundary layer flows are ubiquitous in vehicles transiting through fluid mediums. The interaction of turbulent boundary layers with vehicle surfaces, rotors, propulsors, and fans excite unsteady forces over the vehicle and blade surfaces. The unsteady forces radiate to the far field as acoustic sound with their spectral form and intensity dependant on the turbulence energy and surface response. In many practical configurations the boundary layers are under the effects of curvature and pressure gradients, for example boundary layers developed over the surface of a vehicle and then ingested into a rotor such as in many pusher, Vertical Take-Off and Landing (VTOL) rotorcraft, submarines, small Unmanned Aerial Vehicles (UAV's), and Unmanned Underwater Vehicles (UUV's). Typically these shear layers are also under the influence of some form of pressure gradient induced by the vehicle body surface. This paper will examine the formulation of an acoustic prediction model that has been used to some success and then expound the usage of isotropic turbulence models and Taylor's frozen flow hypothesis in the determination of the two point velocity correlation function. The methods used to take measurements will be discussed and then comparisons between correlation functions using the full two point correlation function and that determined from Taylor's frozen flow hypothesis will be shown.

A. Acoustic noise predictions in turbulence

Glegg et al. [1] proposed a time-domain approach with which to analytically predict the far field sound radiated by a rotor ingesting a turbulent boundary layer. In this formulation the overall noise spectrum is given as,

$$S_{pp}(\overline{x},\overline{\omega}) = \frac{1}{4\pi T}\sum_{n=1}^{B}\sum_{M=1}^{B}\int_{R_{min}}^{R_{max}}\int_{R_{min}}^{R_{max}}\int_{-T}^{T}\int_{-T}^{T} \{arg\}\, dRdR'd\tau d\tau' \tag{1}$$

Where the argument $\{arg\}$ is given in equation 2,

$$\left\{\frac{\partial}{\partial x_i}\frac{n_i^{(n)}(R,\tau)e^{i\omega r^{(n)}(\tau)/c_o}}{4\pi r^{(n)}(\tau)}\right\}\left\{\frac{\partial}{\partial x_j}\frac{n_j^{(m)}(R',\tau')e^{-i\omega r^{(m)}(\tau')/c_o}}{4\pi r^{(m)}(\tau')}\right\} R_{FF}^{(n,m)}(R,R',\tau,\tau') \tag{2}$$

R_{FF} is the unsteady loading correlation function which can be found from the correlation function of the upwash velocity in the following manner,

$$R_{FF}^{(n,m)} = \int_{-\infty}^{\tau}\int_{-\infty}^{\tau} s(R,\tau-\tau_o)s(R',\tau'-\tau_o)R_{ww}^{(n,m)}(R,R',\tau_o,\tau_o')d\tau_o d\tau_o' \tag{3}$$

Where $s()$ is the Kussner function and $R_{ww}^{(n,m)}$ is the correlation function of the upwash velocity. Finally the upwash velocity can be determined from the measured two point space-time correlation function of the inflow turbulence.

$$R_{ww}^{(n,m)}(R,R',\tau_o,\tau_o') = n_i^{(0)}(R,\tau_m)n_j^{(0)}(R',\tau_m'-s\Delta\tau) R_{ij}(y^{(0)}(\tau_m,R),y^{(0)}(\tau_m'-s\Delta\tau,R'),\tau_m-\tau_m') \tag{4}$$

From this the far field sound spectrum can be computed knowing just the rotor geometry and the inflow turbulence correlation function. Measuring the full four dimensional two point correlation function can often be exhaustive so methods of predicting its form with limited measurements have been used in acoustic predictions. Two methods used include assuming isotropic turbulence (making the definition of $R_{ww}^{(n,m)}$ trivial), and using Taylor's frozen flow hypothesis to relate two point statistics from single point statistics. In this case a turbulence profile is measured using a hot wire anemometry setup. Taylor's hypothesis is then used to compute the two point correlation function from the single point statistics captured by the hotwire measurements.

The integral length scales of the flow $l_p(\omega)$ have been traditionally estimated using the integral time scales. This can be done by assuming Taylor's frozen flow hypothesis; that the turbulence within the flow is frozen and convected along at a constant convection velocity, U_c. In general this convection velocity has been found to be approximately the local mean velocity. This finding falls off once the boundary layer moves into the inner region and large scale effects diminish as described by Renard and Deck [2]. The single point correlation function can be found using the equation below,

$$\rho_{u_s u_s}(x, y; \Delta x_s) = \frac{\langle u_s(x', y')u_s(x', y', x' - U_s\tau)\rangle}{\sqrt{\langle u_s(x', y')^2\rangle\langle u_s(x', y', x' - U_s\tau)^2\rangle}} \tag{5}$$

The time-scale can be found by integrating the correlation function,

$$\Gamma_{u_s}(x, y) = \int_0^\infty \rho_{u_s u_s}(x, y, \tau)d\tau \tag{6}$$

and the length scales associated with the frozen flow assumption become,

$$L_{st}(x', y') = \Gamma_{u_s}(x, y)U_s \tag{7}$$

To provide a comparison of the correlation function we will use the two point correlation function at two spatial locations to give the actual correlation structure of the flow without assuming frozen flow. This function is given by the following equation,

$$\rho_{u_s u_s}(x, y; \Delta x_s) = \frac{\langle u_s(x, y)u_s(x', y')\rangle}{\sqrt{\langle u_s(x, y)^2\rangle\langle u_s(x', y')^2\rangle}} \tag{8}$$

It should be noted that the mean subtracted data $\langle u_s(x', y')^2\rangle$ in equation 8 is rotor phase mean subtracted rather than overall mean subtracted due to the dependence of this flow field on the rotor phase. The turbulence convection velocity will be estimated by rearranging equation 7 and using the length scale calculated by the two-point correlation such that $U_c = L_s(x', y')/\Gamma_{u_s}(x, y)$. We will compare the two functions and examine the decay rate at various points in the boundary layer. These results will also be compared to the zero angle of attack, axisymmetric case described in Balantrapu et al. [3]. The length scales of the flow calculated using Taylor's hypothesis and the two point correlation function will be compared for each point and the validity of Taylor's hypothesis at various points in the boundary layer discussed. It is expected that the single point correlation function will decay more rapidly than the two point correlation function and that this decay discrepancy will increase as we move towards the inner region of the boundary layer.

II. Experimental Methods

A. Experimental Facility

The wind tunnel used to take the measurements for this analysis is the Virginia Tech Stability Wind Tunnel

(VTSWT) in an anechoic configuration and is shown in Fig. 1. The test section consists of a 1.83 m x 1.83 m x 7.32 m test section enclosed in two kevlar side walls and anechoic floor and ceiling panels. The freestream turbulence levels are less than 0.02 %. Devenport et al. [4] goes into detail of the VTSWT's capability.

Fig. 1 Image of the Virginia Tech Stability Wind Tunnel anechoic test section with the body of revolution mounted. Image is looking downstream

B. Model

The non-axisymmetric flow was produced by a body of revolution pitched at an angle of attack. The body of revolution is shown in Fig. 1 and Fig. 2. It has a diameter of 432 mm and consists of three separate sections that produce specific flow phenomena. The nose is a 2:1 ellipsoid that produces a favorable pressure gradient as the fluid flows past it. The mid-body is a 432 mm diameter cylinder, and the aft section is a 1.17D long section with a 20^0 ramp to induce an adverse pressure gradient.

C. Particle Image Velocimetry

Particle Image Velocimetry was used to examine the velocity field at the aft end of the BOR. The time resolved stereo-PIV plane that was measured is shown in Fig. 2. This setup gave three component velocity fields over a 160 x 160 mm^2 area with a 4.2 mm spatial resolution. The VTSWT is seeded by an MDG seeder that produces atomized Propylene Glycol particles on the order of one micron. The camera's are Phantom v2512 high speed camera's. The laser is a Photonic Industries DM laser with a maximum dual pulse rate of 12.848 kHz. The PIV was taken at the maximum sampling rate in two frame mode to most accurately time resolve the flow.

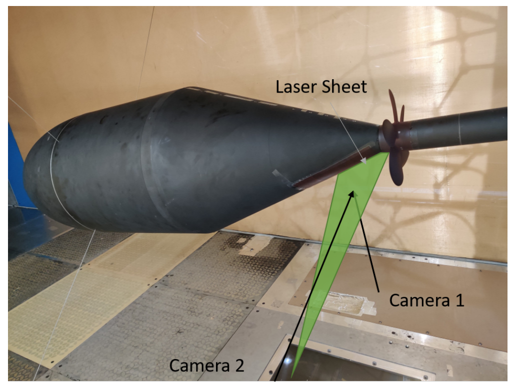

Fig. 2 Measured PIV plane relative to the body of revolution

III. Results and Discussion

The results shown below were taken for a profile at $x/D = 2.97$ for the non-axisymmetric flow case and at $x/D = 2.93$ for the axisymmetric case. The locations of these profiles within the PIV flow fields are shown in Fig. 3 and Fig. 4.

A. Two Point Correlation Structure within the Boundary Layer

Fig. 5 and 6 show streamwise slices of the two-point correlation functions (shown on the vertical axis) for a vertical profile at $x/D = 2.97$ and $x/D = 2.93$ for the non-axisymmetric and axisymmetric flow cases respectively. The horizontal axis is spatial distance from the anchor points

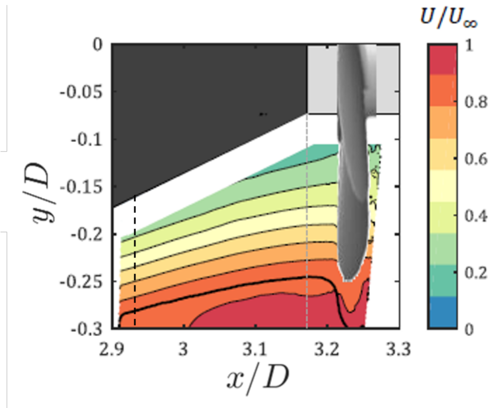

Fig. 3 Boundary layer thickness and mean velocity contours for body of revolution at 0°angle of attack normalized on the freestream velocity.

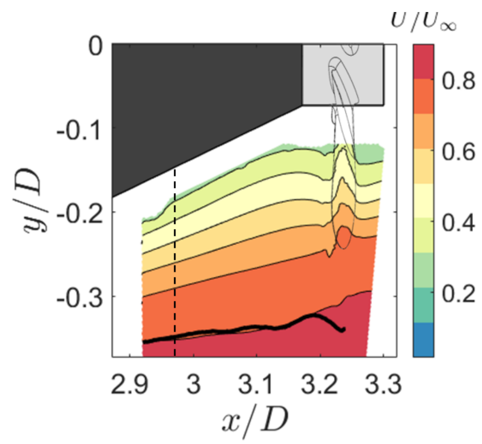

Fig. 4 Boundary layer thickness and mean velocity contours for body of revolution at 5°angle of attack normalized on the freestream velocity.

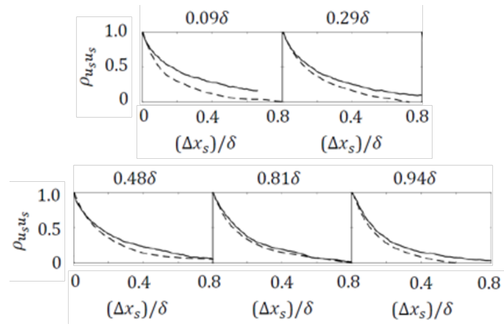

Fig. 5 Comparison of correlation functions for body of revolution at 0°angle of attack [3]

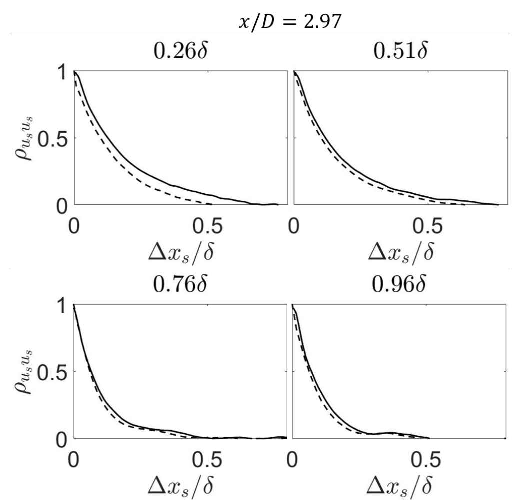

Fig. 6 Comparison of Correlation Functions for body of revolution at 5°angle of attack.

in the streamwise direction. The solid curve is the two-point correlation estimated from the full two-point correlation function in the streamwise direction and the dotted line is the two-point correlation estimated using Taylor's frozen flow hypothesis, assuming a constant convection velocity $U_c = \overline{U_s}$. Comparing the results of Balantrapu et al. [3] to the results obtained in Fig. 6 it is evident that the convection velocity assumed using Taylor's hypothesis is a reasonably good approximation in the outer regions of the boundary layer for both cases.

It can be seen that in both cases the efficacy of Taylor's hypothesis decays beneath a certain point and starts to more significantly underestimate the length scales. There is a general trend that as we move closer to the wall the single point auto-correlations decay faster than the two point correlations. This implies that the turbulence convection speed is greater than the local mean velocity.

To illustrate the decay of Taylor's hypothesis and to determine where it begins to be less accurate, calculations at 41 points in the $x/D = 2.97$ profile were taken and the length scales compared for each of these points as a function of distance from the BOR surface. Fig. 7 illustrates the deficit between the length scales estimated using Taylor's

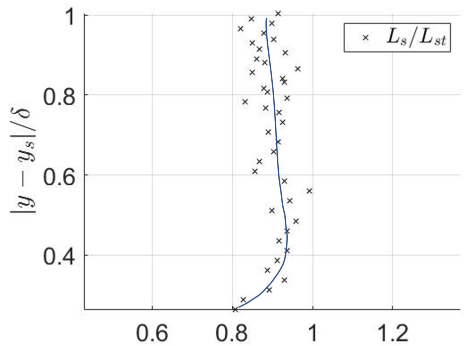

Fig. 7 Comparison of the lengthscales calculated by the measured two point correlation function and those calculated using Taylor's hypothesis and single point statistics.

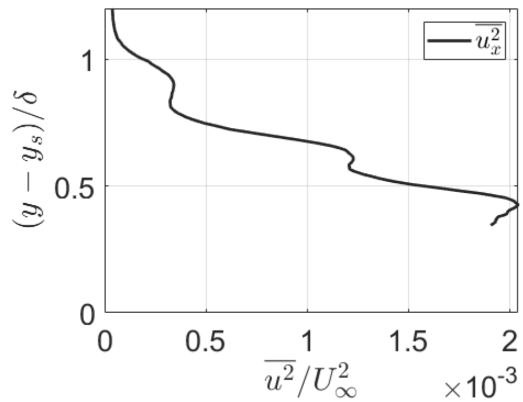

Fig. 8 Turbulence profile of $\overline{u_x^2}$ at $x/D = 2.97$ where y_s refers to the BOR surface.

hypothesis and those found using the two-point correlation function. The vertical axis shows the boundary layer from 0.3δ to δ and the horizontal axis shows the ratio between the two quantities (L_s/L_{st}). A 5^{th} order polynomial was fit to the data. In the outer region of the boundary layer Taylor's hypothesis under predicts the length scales by around 10% with a fairly significant variance around the data fit. The peak turbulence shown in Fig. 8 occurs at around $|y - y_s|/\delta = 0.44$ and coincides with the maximum value of the fit curve. Below this point Taylor's hypothesis appears to decline, however due to the lack of a significant number of good data points below $|y - y_s|/\delta = 0.3$ we can not conclude that this trend will continue.

To visualize the evolution of the flow correlation structure five anchor points (corresponding to those shown in Fig. 6) were chosen and the two-point correlation plotted in Fig. 9. As the anchor points move towards the surface of the BOR the correlation structure elongates in the streamwise direction and rotates anticlockwise to become more aligned with the BOR ramp. Outside the boundary layer the two-point correlation rapidly decays to zero due to the lack of significant correlated structures.

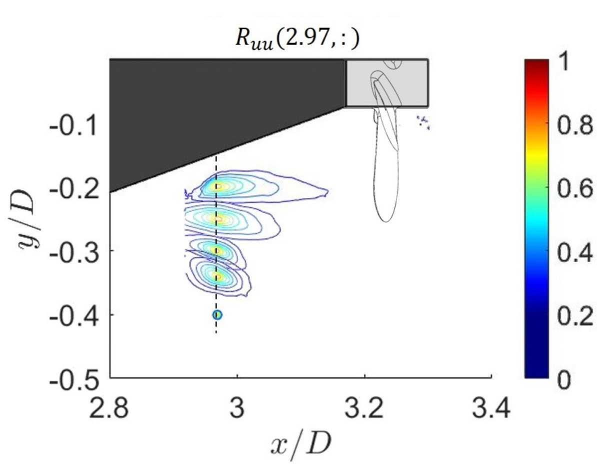

Fig. 9 Evolution of the two-point correlation structure throughout the boundary layer.

B. Two Point Correlation Structure in the Rotor Plane

Fig. 10 shows the correlation structure at the rotor inlet for both the 0°angle of attack, and the 5°angle of attack case. The correlation structure is stretched in the streamwise direction and the major axis is rotated 18°clockwise from the horizontal (or 38°from the BOR ramp surface). Comparing the turbulence structure for the axisymmetric configuration in Fig. 10b to the data shown in Fig. 10a we see an increase in the rotation of the correlation structure. The inclination of the BOR increases the strength of the ADP along the aft ramp and further distorts the turbulence resulting in the structure seen in Fig. 10a.

Taylor's frozen flow hypothesis holds up reasonably well at this location, as indicated by Fig. 11. The convection velocity at 0.5δ is approximately $U_c = 14.63 m/s$ and Taylor's hypothesis results in a length scale of $L_{st} = 1.06 L_s$.

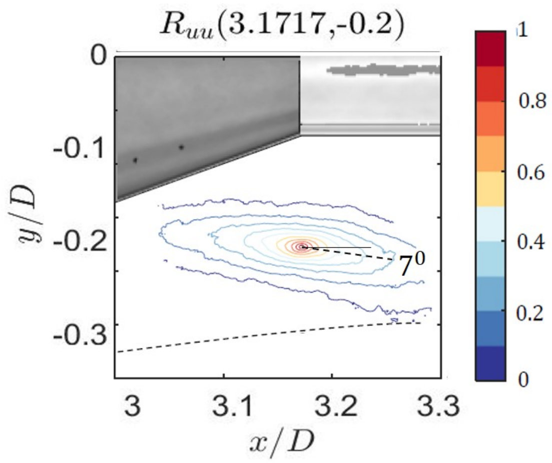

(a) 0°angle of attack flow case

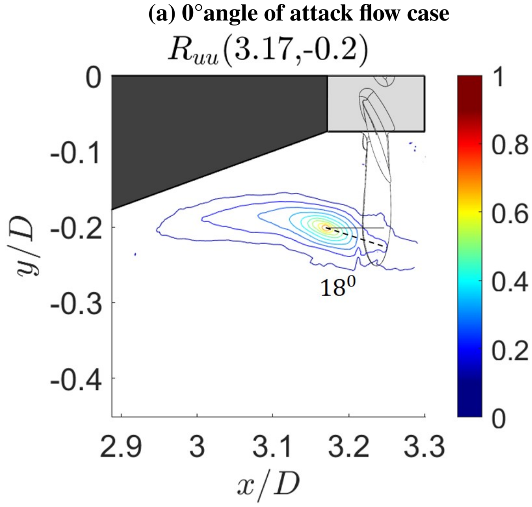

(b) 5°angle of attack flow case

Fig. 10 Two point correlation functions computed from the PIV results at the rotor inlet and approximately halfway into the boundary layer

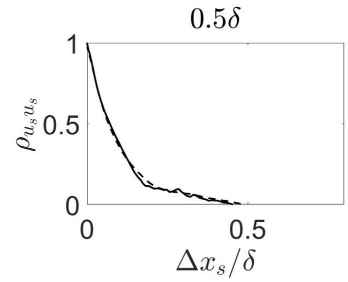

Fig. 11 Comparison of single and two point correlation functions

IV. Conclusion

The correlation structure for a non-axisymmetric boundary layer was examined and it's evolution as a function of distance from the surface was shown. It was found that the correlation structure stretched in the streamwise direction and rotated anti-clockwise as the anchor points moved towards the surface of the BOR. Taylor's frozen flow assumption as a means of estimating length scales was shown to be fairly good for the outer regions of the boundary layer but tended to consistently underestimate the length scales by about 10 %. It's efficacy was shown to peak with the turbulence and then decay as it moved closer to the wall. The correlation structure at the rotor plane was also examined and compared to the axisymmetric case. It was found to be rotated clockwise 11^0 relative to the axisymmetric case and Taylor's hypothesis was shown to estimate the length scales quite well at this location.

Acknowledgments

The author would like to thank the Office of Naval Research for sponsoring this work under grants N00014-17-1-2698 and N00014-17-1-2682, specifically Drs. Ki-Han Kim and John Muench. Further acknowledgements go to Vidya Vishwanathan, Shishir Damani, Rachel Andrews, Aayush Salot, and Shivam Khullar amongst others for their assistance during the wind tunnel experiments. The author would also like to thank Mr. Michael Marcolini for his ever present advice.

References

[1] Glegg, S. A. L., Devenport, W., and Alexander, N., "Broadband rotor noise predictions using a time domain approach," *Journal of Sound and Vibration*, Vol. 335, 2015, pp. 115–124. https://doi.org/10.1016/j.jsv.2014.09.007.

[2] Renard, N., and Deck, S., "On the scale-dependent turbulent convection velocity in a spatially developing flat plate turbulent boundary layer at Reynolds number," *Journal of Fluid Mechanics*, Vol. 775, 2015, pp. 105–148. https://doi.org/10.1017/jfm.2015.290.

[3] Balantrapu, A. N., Hickling, C., Alexander, N., and Devenport, W., "The structure of a highly-decelerated axisymmetric turbulent boundary layer," 2021.

[4] Devenport, W. J., Burdisso, R. A., Borgoltz, A., Ravetta, P. A., Barone, M. F., Brown, K. A., and Morton, M. A., "The Kevlar-walled anechoic wind tunnel," *Journal of Sound and Vibration*, Vol. 332, No. 17, 2013, pp. 3971–3991. https://doi.org/10.1016/j.jsv.2013.02.043.